ACADEMIC PRESS

Available online at www.sciencedirect.com

SCIENCE DIRECT®

Icarus 161 (2003) 157–163

ICARUS

www.elsevier.com/locate/icarus

First experimental studies of large samples of gas-laden amorphous "cometary" ices

Akiva Bar-Nun* and Diana Laufer

Department of Geophysics and Planetary Sciences, Tel Aviv University, Ramat-Aviv, Tel-Aviv, 69978, Israel

Received 20 May 2002; revised 15 August 2002

Abstract

In a unique machine, the first of its kind, large (200 $cm^2 \times 10$ cm) samples of gas-laden *amorphous* ice were prepared at 80 K and 10^{-5} Torr. The sample consisted of a fluffy agglomerate of 200-μm ice grains, similar to what is presumed to be the structure of comet nuclei. The sample was heated from above by IR radiation. The properties studied were gas content in the ice and its emanation from the ice upon warming and bearing on the gas/water vapor ratio observed in cometary comae vs this ratio in cometary nuclei and the effect of internal trapped gas on the thermal conductivity of the ice and the density and mechanical properties of pure ice vs gas-laden ice. These findings might have significance for the interpretation of comet observations, the forthcoming ESA's Rosetta space mission to Comet 46P/Wirtanen in 2012, and to other comet missions.

Keywords: Comets; Comets, composition; Ices; Surfaces, comets; Thermal histories

I. Introduction

It is well accepted now that comets delivered a large fraction of water, organics, and gases to the forming Earth. This is based mainly on the D/H ratio in cometary water, which is only two times larger than the mean value in ocean water, but 10 times larger than this value in the solar nebula in which Earth was formed (Eberhardt et al., 1995). This suggests that the water in cometary ices, highly enriched in HDO, originated in the collapsing intersellar cloud, in which HDO is highly enriched, but it did not fully equilibrate with the hydrogen and deuterium in the solar nebula (Laufer et al., 1999). Moreover, the ratios of Ar/Kr/Xe in the atmospheres of Earth and Mars are entirely different than the solar values (Owen and Bar-Nun, 1993). These noble gas ratios can be obtained when these gases are trapped preferentially in the forming cometary ices, when water vapor freezes into ice at ~25 K in their presence (Notesco and Bar-Nun, 2002). The Giotto and Vega missions to Comet Halley as well as the observations of Comets Hyakutake and Hale–Bopp enlarged enormously our understanding of the importance of comets to Earth's volatile inventory. Hopefully, the Stardust and Rosetta missions will widen this knowledge.

In numerous experiments on 0.1–100-μm thick ice samples, formed by flowing water vapor and CO onto a cold surface, it was found that CO is trapped in the ice only when the ice is formed in its amorphous state, below 120 K (Bar-Nun et al., 1985, 1987; Laufer et al., 1987; Notesco and Bar-Nun, 1997). Therefore more than 10% of gas/water, mostly CO, in comets such as Halley, Hyakutake, and Hale–Bopp, suggests that their ice was formed in the amorphous state. (Comet C/1999 S4 Linear's low CO/H_2O ratio has still to be explained (Bockelée-Morvan et al., 2001)). At these temperatures, the water molecules stick to each other wherever they fall, not having enough energy to reorder into the crystalline structure. This results in an open amorphous ice structure into which the gas molecules can enter. They stay there for some time depending on the temperature, due to van der Waal forces or hydrogen bonds, until another ice layer covers the pores in which they reside (Notesco et al., 1999). Beginning at about 120 K, the water molecules have enough energy to move and form the more stable cubic form

* Corresponding author.
E-mail address: akivab@luna.tau.ac.il (A. Bar-Nun).

0019-1035/03/$ – see front matter © 2003 Elsevier Science (USA). All rights reserved.
PII: S0019-1035(02)00016-7

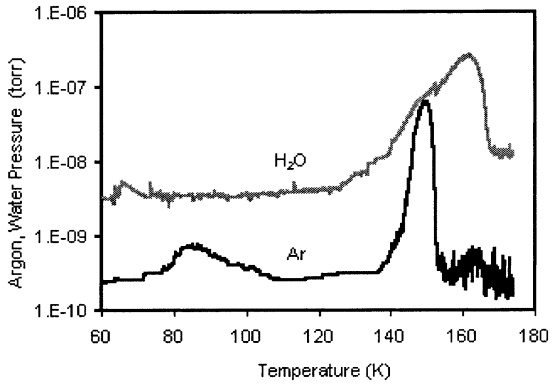

Fig. 1. Gas evolution from a 0.1-μm amorphous gas-laden ice sample upon its warming up. The gas comes out when the amorphous ice transforms into its crystalline and "restrained amorphous" forms.

with about 70% remaining as "restrained amorphous" ice (Jenniskens and Blake, 1994). The rate of transformation increases exponentially and becomes very large at ~135 K. During this process, the gases that were trapped in the amorphous ice can be released from it by dynamic percolation (Laufer et al., 1987) following the increasing fraction of transformed ice. An experimental example of gas release during this transformation is shown in Fig. 1, where all the trapped Ar is released during the transformation to both cubic and "restrained amorphous" ice. When comets, formed as an agglomerate of particles of gas-laden amorphous ice plus silicates and heavy organics, either in the Kuiper Belt or in the Uranus–Neptune region from which they were ejected into the Oort cloud, come close to the Sun, their upper layer is heated.

When this upper ice layer reaches 120 K it begins to transform into cubic ice and into restrained amorphous ice, accelerating at 135 K and releasing the trapped gases. Moreover, the heat of crystallization $\sim 9 \times 10^8$ erg g^{-1} (Ghormley, 1968) may propagate partially inward, transforming deeper layers and releasing more gas from the interior. This process can account for cometary bursts well beyond perihelion, for cometary crater formation and jets, and for the breakdown of comet nuclei (Prialnik and Bar-Nun, 1992; Prialnik, 1997).

To cover the gap between the physics of the well-studied very thin (0.1–100 μm) ice samples and real comet behavior, an intermediate experiment is needed. The first large-scale experiment was the KOSI experiment, which produced remarkable experimental results on heat conduction, compressive strength, the ejection of dust grains, density, and bulk properties. In this experiment, a fine spray of a slurry of liquid water with silicate particles was sprayed into liquid nitrogen. The ice formed was crystalline (Grün et al., 1991, 1993). To add gas to the sample, CO_2 was also sprayed into the liquid nitrogen. This resulted in a mixture, at 80 K, of minerals covered by crystalline ice and mixed with frozen CO_2. The next logical step in studies of large ice samples should be production by vapor deposition of a large sample of *gas-laden amorphous ice*, since observations of comet behavior suggest that their ice is initially amorphous and traps gases in its open structure.

II. Experimental

One cannot produce large samples of amorphous ice by depositing water vapor on a cold plate, as is done routinely with up to hundreds of micrometer thick ice samples in all small ice sample studies. This is because one has to get rid of the large heat of condensation of water vapor into ice (2.7×10^{10} erg g^{-1}) through the growing ice sample, whose heat conductivity is poor (less than $\sim 10^4$ erg cm^{-1} K^{-1} s^{-1}). If one grows an ice layer too thick, the heat of deposition cannot be transmitted to the cold surface and the newly deposited ice layer reaches ~120 K and becomes crystalline rather than amorphous and, consequently, does not trap in it the gas which is flowed together with the water vapor. The solution was to slowly form thin ~200-μm ice layers on a 80 K (liquid nitrogen) cold plate, through which the heat of condensation of water could still be transmitted to the cold surface, remain amorphous, and trap the accompanying gas in it. Once a thin amorphous gas-laden ice layer is formed, it is scraped from the plate on which it was formed by a 80 K cold knife into the sample container, which is covered by a dome.

All these parts, as well as the heat shield surrounding the entire chamber, are kept at 80 K by a controlled flow of liquid nitrogen. This fully automatic, hydraulically controlled, process is repeated at 10^{-5} Torr for about 10 to 20 h until a large enough ice sample is accumulated, namely 200 cm^2 and 5–10-cm high sample of an agglomerate of 200-μm particles of amorphous gas-laden ice. The sample is then covered by the 80 K deposition plate while the dome is heated to ~330 K. When the plate is removed, the sample is irradiated from above by the heated irradiating dome, made of a rough surfaced aluminum, at better than 3% uniformity. The IR flux from the irradiation dome, 5×10^5 erg cm^{-2} s^{-1}, was calculated as a black body radiation at 330 K. Since water is almost black to IR at the 330 K black body spectrum, the energy input of the irradiation dome is totally absorbed by the upper layers of the ice sample.

Ten thermocouples (types E and T) are embedded in the ice, recording the temperature profile in the ice. A mass spectrometer (Farran Scientific Micropole Sensor, Model MPA CF-10) records the emanation of gas and water vapor from the heated sample, through a 2-cm hole in the dome right above the center of the sample. The manufacturer-provided sensitivity to various gases was checked by analyzing mixtures of gases with known compositions.

The ice density was measured by collecting a small ice sample in a 1 cm^2 × 10-cm glass vial simultaneously with the large ice sample and measuring its volume at 80 K and again when melted.

The compressive strength was measured by forcing a

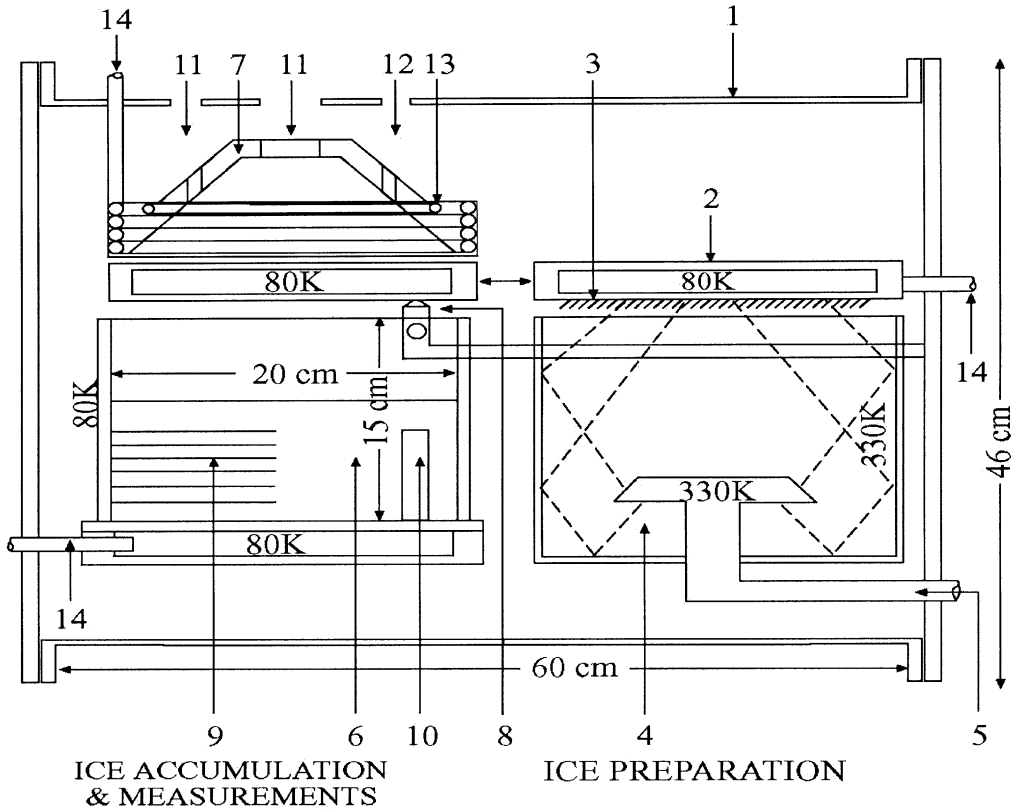

Fig. 2. A schematic drawing of the machine producing large (200 $cm^2 \times 10$ cm) gas-laden amorphous ice samples, as a "comet" simulation: (1) vaccum chamber; (2) cold plate at 80 K; (3) 200-μm amorphous gas-laden ice; (4) homogeneous flow of water vapor and gas; (5) water vapor and gas pipes; (6) 200 cm^2 and 5–10-cm thick ice sample; (7) heating dome; (8) 80 K cold knife; (9) thermocouples; (10) density measurements; (11) mass spectrometer; (12) ionization gauge; (13) heating tape; (14) LN_2 cooling pipes.

force-meter penetrator (Extech Instr. Model FG 5000) cooled to 80 K into the ice, immediately after the experiment was terminated and the chamber was opened. A schematic drawing of the machine is presented in Fig. 2.

As to pumping, the ambient pressure in the chamber was maintained during the deposition at 10^{-5} Torr by an Alcatel MPD-5010 molecular drag pump and an Alcatel 5080–5001 turbo-molecular pump, backed by a Welch Duo-seal 1402 rotary pump. In addition, the $\sim$1 m^2, 80 K, radiation shield acts as a pump for water vapor, but not for Ar, which does not freeze at 80 K. This resulted in an ambient Ar pressure about a 100 times larger than the ambient water pressure throughout the sample preparation stage.

Yet, as shown in Fig. 4, at the onset of heating, the Ar flux responds very fast, *well above* its high ambient level. It also decreases, though more slowly, when the heating dome is blocked. Thus all the variations in the Ar flux represent changes in flux well above the ambient Ar background.

III. Experimental results

A. Gas trapping and release

To test whether we indeed produced a sample of amorphous ice we used argon, flowing together with the water vapor onto the 80 K cold deposition plate, as well as flowing only argon onto the plate. As expected, it was found that argon does not freeze on the 80 K cold plate. However, when flowed together with water vapor that condensed on the cold plate, it was trapped in the forming amorphous ice. As found in thin ice samples, CO behaves like argon (Bar-Nun et al., 1987).

In two experiments, a 200-cm^2 and 0.5-cm thick ice sample was produced. During its irradiation by the heating dome, the flux of emanating water vapor and argon were monitored by the mass spectrometer until all the ice sample sublimated. The mass-spectrometer record of H_2O and Ar during the entire experiment is shown in Fig. 3.

Several interesting results come out of this experiment: (1) As stated above, argon was trapped in the 80 K ice, whereas it was not frozen on the cold plate when flowed alone onto it. This shows definitely that the ice formed by this method is amorphous, since only amorphous ice traps argon in it while being formed. (2) The integrated mass-spectrometer records of argon and water are Ar/H_2O = 1.01, whereas in the flowed mixture it was 1:1; hence all the argon was trapped in the amorphous ice. (3) The timing of argon evolution from the ice, as seen in Fig. 3, is of prime importance for the interpretation of comet observations:

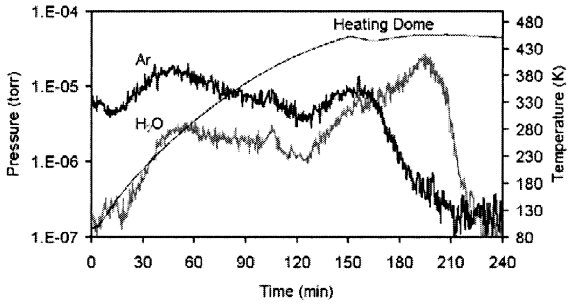

Fig. 3. Evolution of argon trapped in the ice and ice sublimation, upon heating from above. Note the early rise of the argon and its *exhaustion* before all the ice sublimates.

even in a 0.5-cm thick ice layer heated from above, the argon flux (which behaves exactly like CO) rises to a level about seven times higher than that of the water vapor. This is because the argon leaves the amorphous ice when it transforms into the cubic and "restrained amorphous" forms, as was found in numerous studies of thin ice samples. This process goes on in the interior of the ice sample, supplying gas to the experimental "coma." However, the heated ice layer is eventually exhausted of its gas, as can be seen in Fig. 3. The argon flux declines well before all the water ice sublimates. This raises the question of what does the gas/H_2O ratio in cometary comae tell us about this ratio in the nuclei.

B. Thermal behavior and gas emanation from the ice

In Fig. 4 is shown the thermal history of a 6-cm thick ice sample through five thermocouples and the mass-spectrometer records of water and argon emanation. At 812 min (after the beginning of deposition of the ice) the ice sample was exposed to the 330 K heating dome.

As expected, the temperature of the ice rose very steeply on the surface and more sluggishly below the surface. This allows the determination of the thermal conductivity of the ice. When the heating dome was blocked at 858 min, the surface temperature dropped immediately whereas the deeper layers lagged. Although the Ar/H_2O ratio in the ice sample was 1:1, upon heating, the Ar/H_2O ratio in the emitted gas rose to ~10. When the heating dome was blocked, the water flux, which comes out of the surface, dropped immediately, whereas the drop in the argon flux lagged. The same holds, of course, for the renewal of the heating, at 868 min. Again, the gas/water ratio in the coma was not its value in the nucleus.

The thermal conductivity of the 0.25 g cm^{-3} (see below) amorphous ice layer can be calculated from the temperature profiles of the thermocouples embedded in the ice sample, such as in Fig. 4. The heat conduction coefficients of amorphous and cubic water ice were calculated by Klinger (1980) to be 2–3 $\times$ 10^4 and 2.8 $\times$ 10^5 erg cm^{-1} K^{-1} s^{-1}, respectively. In the KOSI experiments, on an agglomerate of hexagonal porous crystalline ice, the derived value of the heat conduction coefficient was 3–6 $\times$ 10^4 erg cm^{-1} K^{-1} s^{-1} (Spohn et al., 1989; Benkhoff and Spohn, 1991; Seiferlin et al., 1996).

In our study, the heat conduction coefficient (K) is calculated for a thick layer of an agglomerate of 200-μm particles with and without trapped argon. The calculation of the heat conduction was made by a scale approximation of the heat diffusion equation. Heat transfer by contact of the ice with the container's walls can be neglected, because the ice sample is surrounded by a mylar sheet, which is decoupled from the 80 K wall of the sample container.

$$\rho Cp_{(ice)} = \frac{\partial T}{\partial t} = \frac{\partial}{\partial x}\left(K_{(ice)} \frac{\partial T}{\partial x} \right), \tag{1}$$

where T is the temperature at level x of the ice sample; t is the time from the beginning of the heating process, which lasts from 2 to 4 h; $0 < x < l$ is the thermocouple's height in the ice layer, where l is the ice sample thickness. The temperature at the bottom of the ice sample ($x = 0$) is constant—80 K, ρ is the measured density of 0.25 g cm^{-3}, and the heat capacity $Cp(T) = 7.49 \times 10^4 T + 9 \times 10^5$ erg g^{-1} K^{-1} is an average between 80 and 120 K (Klinger, 1981). Newer measurements of heat capacity for dense amorphous water ice are almost the same for temperatures of 90–125 K (Handa and Klug, 1988).

The scale approximation of the heat diffusion equation (1) is

$$\rho Cp_{(ice)} \frac{\partial T}{\partial t} = \frac{1}{l^2} K_{(ice)} T. \tag{2}$$

The equation's solution is

$$\ln(T - T_{(x=0)}) = \ln T_{t=0} - \frac{K_{(ice)}}{l^2 \rho Cp} t. \tag{3}$$

The thermal conductivity constant of the very low density

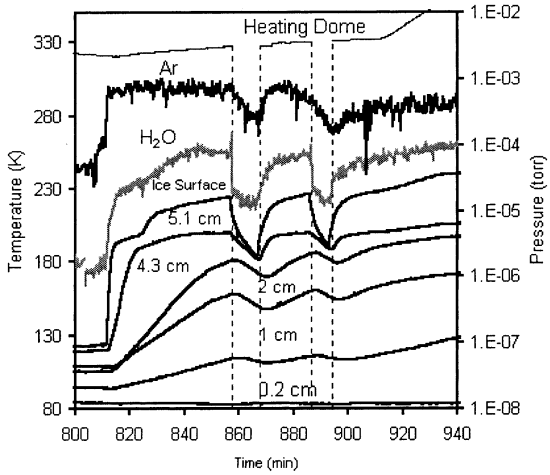

Fig. 4. Temperature profiles of the thermocouples as a function of their distance from the 80 K bottom plate. Note also the sharp decrease and increase of the water flux vs the sluggish-response of the argon emanation, when the ice sample is covered by the cold plate and upon its removal.

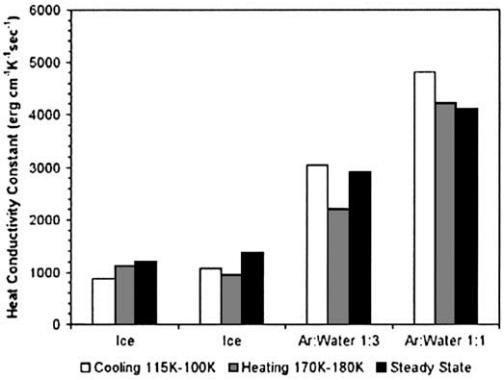

Fig. 5. Heat conductivity constant of various ice samples measured at different temperature ranges.

amorphous ice was derived from the slope of $\ln(T - T_{(x=0)})$ vs time and the calculations were made at three temperature ranges: cooling from 115 to 100 K (not shown in Fig. 4), heating by the dome in the linear range of increase of temperature from 160 to 170 K, and measuring from the time for reaching a steady state at 180 K (Prialnik and Bar-Nun, 1992). Figure 5 shows some of the thermal conductivity values obtained in several experiments. As expected, the thermal conductivity of gas-free ice for the three regions is almost identical, which shows that the calculation method is valid for the three measured temperature ranges.

Yet, the heat conduction of gas-free ice is 30 times smaller than Klinger's value for a block of amorphous ice. This is because our sample is an agglomerate of ~200-μm ice particles and the heat conduction between the grains is poor. One cannot exclude the contribution of water vapor flowing inward to the thermal conductivity. This can be studied in the future, by layering H_2O ice over D_2O ice and measuring the fluxes of H_2O, D_2O, and HDO in the emanating water vapor. It should be noted that we did not detect a harder crust below the surface, as would have been expected if a massive flow of water vapor froze in deeper layers. Nevertheless, a large difference is observed with ice containing gas. The thermal conductivity of gas-laden ice is much higher, and more so when the gas content is even higher (Ar: H_2O = 1:3 vs 1:1). This immediately demonstrates the importance of the trapped gas in the conduction of heat into the interior of comets. It also explains the decrease in thermal conductivity when the gas content in the ice decreases during heating and shows that water vapor flowing among the loosely bound ice particles does not convey much heat.

C. Mechanical properties

Our ice is a loose agglomerate of ~200-μm ice particles, scraped from the deposition plate. Its measured density, as mentioned above, is 0.25 g cm^{-3}. It does not contain mineral or organic dust. An agglomerate of small ice grains is a good simulation of cometary nuclei, which were presumably formed by the slow agglomeration of gas-laden amorphous ice grains and whose density with 50% of silicates and heavy organics was calculated for Comet Halley by Rickman (1989) to be 0.3–0.7 g cm^{-3} and for Comet Borrelly to be 0.29–0.83 g cm^{-3} (Farnham and Cochran, 2002).

The measurement of mechanical properties is simple but rather hard to interpret. Pressing a force meter cooled to 80 K into the extremely fluffy ice produced the results shown in Fig. 6. As the ice is compressed, its compressive strength increases, while its open spaces decrease. Pure ice is "stronger" whereas the argon trapped in the ice "weakens" it, since the ice particles, which form the sample, are fluffier. It does, however, reach a finite value. We also observed in our experiments that during heating, when the argon left the ice, the fine ice structure collapsed.

A very low compressive strength of ~2 $\times$ 10^5 dynes cm^{-2} can be deduced from our experiments. For comparison, in the KOSI experiments, in which mineral grains were mixed with hexagonal ice grains or covered by a layer of hexagonal ice, the compressive strength was 3 $\times$ 10^5–2 $\times$ 10^7 dynes cm^{-2}, depending on the mineral content (Jessberger and Kotthaus, 1989). This means that finally, when everything in pure ice is compressed enough, the compressive strength reaches a value of 2–3 $\times$ 10^5 dynes cm^{-2} and that mineral dust can increase the compressive strength by two orders of magnitude. Anchoring a drilling platform on a comet surface, for obtaining a core sample as initially suggested for Rosetta (Hilchenbach et al., 2000), might thus be a major engineering problem.

IV. Discussion

By trapping 1:1 Ar:H_2O in the slowly deposited ice at 80 K, it was proven that the ice is amorphous, since Ar does not freeze at 80 K. Large samples of 200 cm^2 $\times$ 10 cm, of an agglomerate of 200-μm ice particles of this amorphous gas-laden ice, were produced. These samples can represent

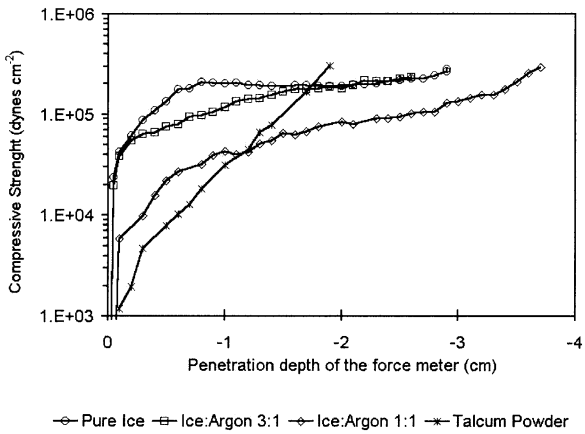

Fig. 6. Compressive strength of the studied ice samples as function of the penetration depth in the ice.

pristine cometary nuclei and their still unprocessed interiors. Yet, we should remember that the ice samples did not contain mineral and organic dust and, consequently, the build-up of an insulating dust layer and its subsequent effect on the penetration of the heat wave could not be studied.

The most important finding was that the ratio of Ar/water vapor in the experimental "coma" was between 7 (Fig. 3) and 10 (Fig. 4) times larger than the Ar/ice ratio in the experimental "nucleus." In the 0.5-cm thick samples, the Ar was exhausted from the ice well before the ice sublimated completely (Fig. 3) but in the 6-cm thick sample, Ar kept emanating from deeper layers (Fig. 4). This observation has direct bearing on the correlation between the gas water vapor observed in cometary coma and the gas/ice ratio in the nucleus.

As to the physics of gas release: in each amorphous ice grain, gas is trapped in closed pores and can leave them by a dynamic percolation process (Laufer et al., 1987) only above 120 K, when the water molecules have enough energy to move and form the more stable cubic form, with about 70% of "restrained amorphous" ice (Jenniskens and Blake, 1994), which also releases the gases trapped in the amorphous ice (Fig. 1). The rate of transformation increases exponentially and becomes very fast at 135 K, as seen by the evolution of Ar in Fig. 1. Also seen in Fig. 1 and 3 is the small increase in water flux when water molecules are carried by the outflowing Ar. One should also note in Fig. 1 that the Ar is exhausted well before the 0.1-μm ice layer is completely sublimated, as in the 0.5-cm ice layer in Fig. 3.

Once the gas leaves each grain, it still has to find its way out, again by dynamic percolation, through the agglomerate of ice grains. The density of the ice sample was found to be 0.25 g cm^{-3}. If the density of each 200-μm ice grain is close to 1 g cm^{-3}, three fourths of the structure is void, much more than in a closely packed pile of marbles. This fluffiness is seen also by the low compressive strength in Fig. 6, which decreases even more when gas is trapped in the ice. This apparently means that with trapped gas, each ice grain has a density lower than 1 g cm^{-3}.

Yet, even this fluffy structure requires dynamic percolation for the gas molecules to migrate all the way to the surface. Thus during this process, the voids are filled with gas which transmits the heat better than the ice bridges between the ice grains, resulting in the very large increase in the thermal conductivity of gas-laden ice compared with pure ice, as seen in Fig. 5. Since Ar, like CO, does not freeze even at the lowest temperature—80 K, we do not expect it to migrate inward, and the increase in the thermal conductivity is attributed only to gas-filled voids. The exothermicity of the transformation 9×10^8 erg g^{-1} (Ghormly, 1968) also contributes to the propagation of the heat wave inward (Prialnik and Bar-Nun, 1992) but to a much lesser extent than the gas, as seen in Fig. 5.

How would all this affect the release of CO and other gases from the various layers of a comet nucleus? One can look at the 6-cm sample shown in Fig. 4 as an example: As the heat wave moves inward, deeper layers reach the ~120 K transformation temperature and the gas trapped in each ice grain in these layers is released into the voids and tries to escape to the surface. When the IR irradiation is stopped, the water vapor, which comes only from the surface drops immediately, whereas the response of the Ar is sluggish. This is because the deeper layers still release their trapped gases and the entire structure is still filled with gas. (In subsequent experiments we plan to stop the heating for a longer period and see to what level would the Ar flux drop, along with the temperatures of the deeper layers.)

Thus, gas comes out from the entire transforming ice structure, through dynamic percolation, whereas the water vapor comes only from the surface. This explains the 7 to 10 times larger gas/water vapor ratio in the experimental "coma" than the gas/ice ratio in the nucleus. Therefore, the ~10% of CO to water vapor seen in the comae of Comets Halley, Hyakutake, and Hale–Bopp might well mean that the CO/ice in these nuclei could be closer to 1%.

In cometary nuclei, when the ice sublimates, it leaves behind a dust layer, whose poor thermal conductivity stops the heating and the emanation of gas and water vapor. When gas pressure builds up in deeper layers, explosions can occur, which remove the dust layer and form a crater with clean ice, which can be heated further. This is equivalent to our blocking the irradiation, and lowering of the temperature of the sample, which resulted in a decrease in the Ar and water vapor flux, as well as their renewal when the irradiation was resumed (Fig. 4). A similar event was probably responsible for the leveling off of both water vapor (OH) and CO, as well as most other gases emanating from Comet Hale–Bopp at about 3 AU pre-perihelion and the sharp increase at about 2 AU pre-perihelion (Biver et al., 1997). Also, in this case, the CO flux at 5.2 AU pre-perihelion was approximately six times *larger* than the water flux, but if became approximately five times *smaller* than water at perihelion. Apparently, the upper layers were exhausted and gases came out only, and more slowly, from deeper layers. A model incorporating all our new results is now being prepared.

Last but not least, the low density and compressive strength, which attest to the fluffy structure of the ice, should be of concern for the Rosetta lander. However, incorporating about 25% of mineral dust and about 25% of organic CHON particles, as found for Comet Halley, will possibly somewhat harden the surface.

Acknowledgments

This project was supported by the Deutsche Forschungsgemeinschaft, the Israel Science Foundation Grant 194/93-2, and the Adler Fund for Space Research and the United States–Israel Binational Science Foundation Grant 2000005. We acknowledge with thanks helpful discussions with L. Alperovich and G. Notesco.

References

Bar-Nun, A., Herman, G., Laufer, D., Rappaport, M.L., 1985. Trapping and release of gases by water ice and implications for icy bodies. Icarus 63, 317–332.

Bar-Nun, A., Dror, J., Kochavi, E., Laufer, D., 1987. Amorphous water ice and its ability to trap gases. Phys. Rev. B 35, 2427–2435.

Bar-Nun, A., Kleinfeld, I., Kochavi, E., 1988. Trapping of gas mixtures by amorphous water ice. Phys. Rev. B 38, 7749–7754.

Benkhoff, J., Spohn, T., 1991. Thermal histories of the KOSI samples. Geophys. Res. Lett. 18, 261–264.

Biver, N., 22 colleagues, 1997. Long-term evolution of the outgassing of Comet Hale–Bopp from radio observations. Earth, Moon, Planet 78, 5–11.

Bockelée-Morvan, D., Biver, N., Moreno, R., Colom, P., Crovisier, J., Gérard, E., Henry, F., Lis, D.C., Matthews, H., Weaver, H.A., Womack, M., Festou, M.C., 2001. Outgassing behavior and composition of Comet C/1999 S4 (LINEAR) during its disruption. Science 292, 1339–1343.

Eberhardt, P., Reber, M., Krankowsky, D., Hodges, R.R., 1995. The D/H and $^{18}O/^{16}O$ ratios in water from Comet P/Halley. Astron. Astrophys. 302, 301–318.

Farnham, T.J., Cochran, A.L., 2002. A McDonald observatory study of Comet 19P/Borrelly: placing the deep space 1 observation into a broader context. Icarus, in press.

Ghormley, J.A., 1968. Enthalpy change and heat-capacity changes in the transformations from high-surface-area amorphous ice to stable hexagonal ice. J. Chem. Phys. 48, 503–508.

Grün, E., Bar-Nun, A., Benkhoff, J., Bischoff, A., Dueren, H., Hellmann, H., Hesselbarth, P., Hsiung, P., Keller, H.U., Klinger, J., 1991. Laboratory simulation of cometary process—Results from first KOSI experiments. In: Newburn, E., Neugebauer, M., Rahe, J. (Eds.), Comets in the Post Halley Era, Vol. 1. Kluwer Academic, Dordrecht, pp. 277–297.

Grün, E., Gebhard, J., Bar-Nun, A., Benkhoff, J., Düren, H., Eich, G., Hische, R., Huebner, W.F., Keller, H.U., Kless, G., Kochan, H., Kolzer, G., Kroker, H., Hührt, E., Lämmerzahl, P., Lorenz, E., Markiewicz, W.J., Möhlmann, D., Oehler, A., Scholz, J., Seidensticker, K.J., Roessler, K., Schwehm, G., Steiner, G., Thiel, K., Thomas, H., 1993. Development of a dust mantle on the surface of an insolated ice-dust mixture: results from the KOSI-9 experiment. J. Geophys. Res. 98, 15091–15104.

Handa, Y.P., Klug, D.D., 1988. Heat capacity and glass transition behavior of amorphous ice. J. Phys. Chem. 92, 3323–3325.

Hilchenbach, M., Kochemann, O., Rosenbauer, H., 2000. Impact on a comet: rosetta lander simulations. Planet. Space Sci. 48, 361–369.

Jenniskens, P., Blake, D.F., 1994. Structural transitions in amorphous water ice and astrophysical implications. Science 265, 753–756.

Jessberger, E.K., Kotthaus, M., 1989. Compressive strength of synthetic comet nucleus sample. In: Hunt, J., Guyenne, T.D. (Eds.), Physics and Mechanics of Comet Materials, Vol. 302. Europ. Space Agency, Paris, pp. 141–146.

Klinger, J., 1980. Influence of phase transition of ice on the heat and mass balance of comets. Science 209, 271–272.

Klinger, J., 1981. Some consequences of a phase transition of water ice on the heat balance of comet nuclei. Icarus 47, 320–324.

Laufer, D., Kochavi, E., Bar-Nun, A., 1987. Structure and dynamics of amorphous water ice. Phys. Rev. B 36, 9219–9227.

Laufer, D., Notesco, G., Bar-Nun, A., 1999. From the interstellar medium to Earth's oceans via comets—An isotopic study of HDO/H_2O. Icarus 140, 446–450.

Notesco, G., Bar-Nun, A., 1997. Trapping of methanol, hydrogen cyanide, and *n*-hexane in water ice, above its transformation temperature to the crystalline form. Icarus 126, 336–341.

Notesco, G., Bar-Nun, A., 2002. Gas trapping in water ice at very low deposition rates and inplications for comets. Icarus, submitted for publication.

Notesco, G., Laufer, D., Bar-Nun, A., Owen, T.C., 1999. An experimental study of the isotopic enrichment in the Ar, Kr, and Xe when trapped in water ice. Icarus 142, 298–300.

Owen, T.C., Bar-Nun, A., 1993. Noble gases in atmospheres. Nature 361, 693–694.

Prialnik, D., Bar-Nun, A., 1992. Crystallization of amorphous ices as the cause of Comet P/Halley's outburst at 14 AU. Astron. Astrophys 258, L9–L12.

Prialnik, D., 1997. A model for the distant activity of Comet Hale–Bopp. Astrophys. J. 478, L107–L110.

Rickman, H., 1989. The nucleus of Comet Halley—Surface structure, mean density, gas and dust production. Adv. Space Res. 9, 59–71.

Seiferlin, N., Komle, I., Kargl, G., Spohn, T., 1996. Line heat-source measurements of the thermal conductivity of porous H_2O ice, CO_2 ice and mineral powders under space conditions. Planet. Space Sci. 44, 691–704.

Spohn T., Benkhoff, J., Klinger, J., Grün, E., Kochan, H., 1989. Thermal histories of the samples of two KOSI comet nucleus simulation experiments. In: Workshop on Analysis of Returned Comet Nucleus Samples. Lunar and Planetary Inst., Houston, pp. 66–67.